The Fifth International Workshop on Micro and Nanotechnology for Power Generation and Energy Conversion Applications
PowerMEMS 2005
Nov. 28-30, 2005
Takeda Hall, The University of Tokyo, Tokyo, Japan

Piezoelectric scavengers in MEMS technology: Fabrication and Simulation

A. Schmitz[1], T. Sterken[1,2], M. Renaud[1,2], P. Fiorini[1], R. Puers[2], C. Van Hoof[1]

[1] IMEC, Kapeldreef 75, B-3001 Leuven, Belgium
Tel.: +32-1628-1194, E-mail: schmitza@imec.be
[2] ESAT, K.U.Leuven, Kasteelpark Arenberg 10, 3001 Leuven, Belgium

Abstract

A robust process flow for fabricating piezoelectric devices in MEMS technology is presented. In this process several devices of different dimensions and electric connections (single and series) are fabricated. The devices range of resonance frequencies is 300-1000 Hz. For the piezoelectric layer two different piezoelectric materials (AlN, PZT) are alternatively used.
Moreover a model for the piezoelectric devices based on finite element calculations is presented. According to calculations with this model the predicted power output of the devices is in the range of 1 - 100 µW

Keywords: piezoelectric scavenger, MEMS, packaging, simulation, model

1 INTRODUCTION

The drive for miniaturization of electronic systems has lead to a research boost in miniature power generators. One class of these generators consists of devices that recycle energy available in the ambient. They are often referred to as scavengers. Typical ambient energy sources are heat or mechanical vibrations. Scavengers can make use of different physical principles to generate electrical power from heat (thermoelectric effect) or from mechanical vibrations (e.g. electromagnetic, electrostatic or piezoelectric principle) [1-5]. An important advantage compared to other power sources like batteries or fuel cells is that scavengers do not rely on a solid or liquid energy storage.
In previous works our group has already successfully developed thermoelectric and electrostatic scavengers [6,7]. In this paper we present the fabrication of a miniaturised vibration scavengers based on the piezo-electric conversion principle.

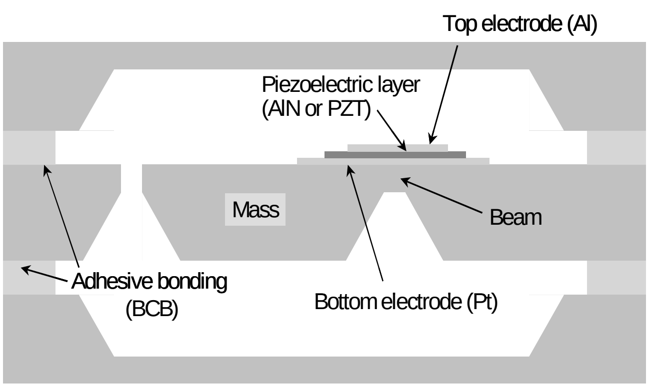

Figure 1: Schematic drawing of the presented piezoelectric scavenger.

2 PIEZOELECTRIC SCAVENGER

Unlike to other approaches the presented type of piezoelectric scavengers is fabricated in silicon using MEMS technology [4,5]. This implies that piezoelectric devices can be fabricated in batch processes, which allows mass production at very low cost.
The design of the presented piezoelectric devices is similar to the classical design of accelerometers and consists of a mass that is attached by a thin beam to the vibrating package (see Figure 1).
The piezoelectric generator is located on top of the beam and consists of a piezoelectric layer sandwiched between a bottom and top electrode. The thickness of the bulk silicon is about 630 µm whereas the beam has a targeted thickness of 25 µm.

Resonance frequency [Hz]	Size of mass [mm x mm]	Length of beam [µm]	Width of beam [µm]
Single piezoelectric devices			
700	3 x 3	2670	3000
1000	3 x 3	3370	3000
700	5 x 5	2240	5000
1000	5 x 5	2830	5000
300	7 x 7	4410	7000
700	7 x 7	2530	7000
1000	7 x 7	1990	7000
Series-connected piezoelectric devices			
700	3 x 3	2670	3000
1000	3 x 3	3365	3000
700	5 x 5	2235	5000
1000	5 x 5	2830	5000

Table 1: Overview of the parameters of the fabricated devices.

Several designs of piezoelectric devices differing in geometry and electrical connection are fabricated on one wafer. The devices are equipped with masses of different dimensions (3x3 mm², 5x5 mm², 7x7 mm²). A variation of resonance frequencies (300 Hz, 700 Hz, 1000 Hz) is realized by varying the length of the beam. The devices are designed as single piezoelectric generators or as a series-connection of four piezoelectric generators. An overview of the variations is given in Table 1.

3 PROCESS DESCRIPTION

3.1 Piezoelectric layer

In the following a robust process flow for fabricating of a fully packaged piezoelectric devices is presented. A schematical overview of the process flow is given in Figure 2.

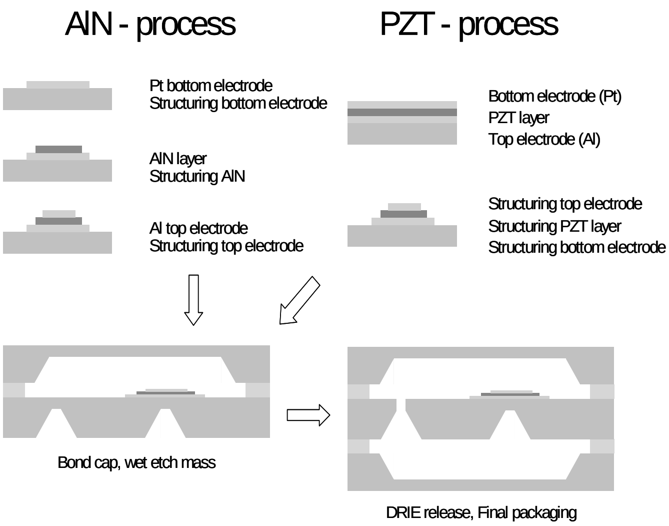

Figure 2: Alternative process flow for piezoelectric scavengers using AlN or PZT as piezoelectric layer.

As piezoelectric material either AlN or PZT (lead zirconate titanate with the composition $PbZr_{0.53}Ti_{0.47}O_3$) are used. Depending on the applied material, the process for depositing the piezoelectric sandwich differs (see Figure 2). In the case of AlN the layers are subsequently deposited and patterned by using a combination of sputtering and lithography. (Figure 2, left). In the other case the bottom electrode, the PZT-layer and the top electrode are first deposited as continuous layers. The PZT layer is deposited by a repeated spinning process of precursors with consecutively pyrolysis and crystallisation steps [8,9]. Subsequently the form of the electrodes and the piezoelectric layer are shaped using etching processes (Figure 2, right).

The advantage of the PZT material are the higher piezoelectric and dielectric constants compared to AlN. However, the deposition of the PZT layer is rather time-consuming as it is deposited in multiple steps. Moreover the sputtering process of AlN is more compatible to a batch MEMS-process.

3.2 Packaging

Next, the top side of the wafer with the piezoelectric devices is protected by a second wafer, bonded to the first by means of BCB, which has been proven to be KOH-resistant. In this way we combine the protection of the wafer during wet etching with the final packaging of the device. Subsequently the thin beam is etched and the mass is released by DRIE-etching.

Finally, a third wafer is bonded under vacuum to the bottom of the wafer with the devices by means of BCB. This packaging concept results in sealed and evacuated piezoelectric generators. Therewith losses due to air damping of the vibrating mass and the beam can be dramatically reduced.

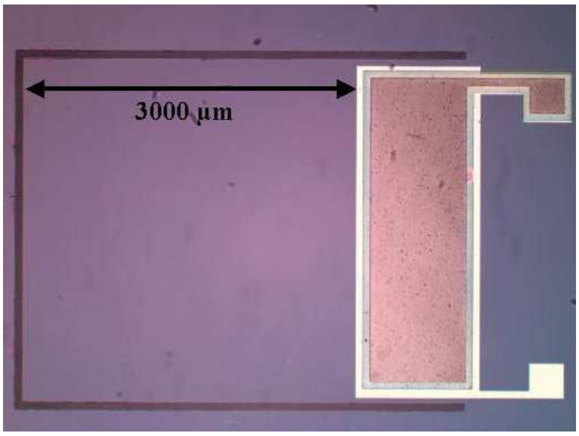

Figure 3.a: Topview of a single piezoelectric generator. The electrodes (top and bottom) and their contact pads as well as the intermediate piezoelectric layer can be clearly seen. The U-shaped perimeter marks the DRIE-etched trench which encompasses the mass (3x3 mm²) and the beam (at the position of the piezoelectric device).

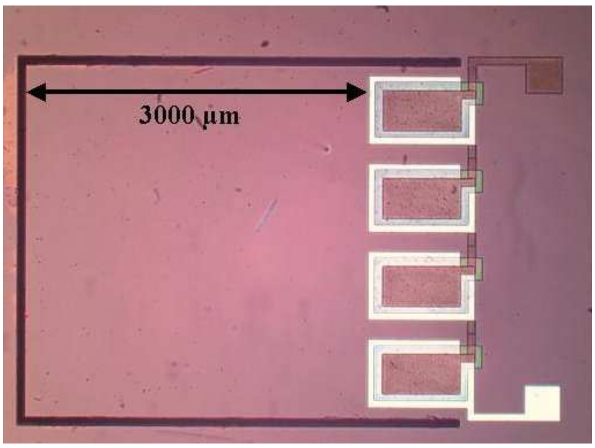

Figure 3.b: Topview of a series-connection of four piezoelectric generators (dimension of the mass: 3x3 mm²).

3.3 Results and status

The fabrication of the devices is currently ongoing. As provisional results, images of a single and series-connected device before the bonding step are shown in Figure 3.a and b.
It is planed to test and characterize the operation of the packaged devices on a shaker at different conditions of excitation frequencies and accelerations.

4 SIMULATION

4.1 Piezoelectric model

Besides the fabrication of piezoelectric scavengers, extensive simulations of the electromechanical behaviour of this scavenger type were carried out using a two-dimensional transient finite element model. The model includes the description of the mechanical strain-displacement relations, the piezoelectric relations between mechanical and electrical quantities as well as the interaction of the piezoelectric device with an external electrical load for the dissipation of the generated electrical power. In the model the device is subdivided in several functional domains on which the respective governing equations are valid (see Figure 4). The governing equations to describe the mechanical and piezoelectric behaviour are based on the principle of virtual work.

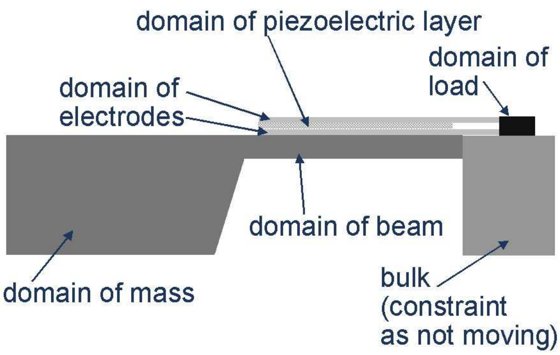

Figure 4: Schematic diagram of the domains of the piezoelectric model.

4.2 Governing equations

The mechanical behaviour in the domains of the beam, mass and electrodes is governed by the mechanical equilibrium equation [10,11]:

$$\int_V \mathrm{T} \cdot \delta \mathrm{S} \, dv = \int_S \mathrm{f}^{S} \cdot \delta \mathrm{u} \, ds + \int_V \mathrm{f}^{B} \cdot \delta \mathrm{u} \, dv \quad , \tag{1}$$

where $\mathbf{T} \in R^{6x1}$ is the the mechanical stress vector, $\mathbf{\delta S} \in R^{6x1}$ is the the virtual mechanical strain vector, $\mathbf{f^S}$ is the surface traction vector, $\mathbf{f^B}$ is the vector of the body force per unit volume and $\mathbf{\delta u}$ is virtual displacement ($\mathbf{f^S}, \mathbf{f^B}, \mathbf{\delta u} \in R^{3x1}$).
In the domain of the piezoelectric layer mechanical and electric quantities interact accordingly to the constitutive equations of the piezoelectric effect [12]:

$$\begin{bmatrix} \mathrm{T} \\ \mathrm{D} \end{bmatrix} = \begin{bmatrix} c^E & e^t \\ e & \varepsilon^S \end{bmatrix} \begin{bmatrix} \mathrm{S} \\ \mathrm{E} \end{bmatrix} , \tag{2}$$

where $\mathbf{S} \in R^{6x1}$ is the mechanical strain vector, $\mathbf{D}$ is the electric displacement vector, $\mathbf{E}$ is the electric field ($\mathbf{D}, \mathbf{E}$ R^{3x1}), c^E is the elasticity matrix, ε^S is the permittivity matrix and e is the piezoelectric matrix. The superscript $(.)^S$ states that the paramter was measured at constant strain and the superscript $(.)^E$ signifies that the parameter was measured at constant electric field.
The interaction between mechanical and electrical properties in the piezoelectric layer is governed by the coupling of the equations for the mechanical equilibrium (Eq-1) and the electrical flux conservation. The equation for the electric flux conservation can be written as [10]:

$$\int_V \mathrm{D} \cdot \delta \mathrm{E} \, dv = -\int_S \rho^s \cdot \delta \Phi^s \, ds \, , \tag{3}$$

where $\mathbf{\delta E}$ is the virtual electric field, ρ^s is the surface charge density and $\delta\Phi^s$ the virtual electric potential on the boundary surface.
The governing equation of the electric behaviour in the domains of the electrodes and the resistor is described by a charge balance:

$$-\nabla \cdot (\sigma \nabla \Phi) = 0 \quad , \tag{4}$$

where σ is the electric conductivity. The charge balance equation is obtained by the equation of continuity in combination with Ohm's law ($\mathbf{j} = \sigma\mathbf{E}$, with $\mathbf{j}$ beeing the current density) and the equation for the electric field ($E = -\nabla\mathbf{\Phi}$). The source and sink terms for electric charges are existent at the boundary surfaces between the electrodes and the piezoelectric layer.

4.3 Results of simulations

Using this model several operation characteristics can be calculated such as output power versus external load and output power versus frequency. Typical shapes of these operation characteristics are shown in Figure 5.a and b.
The developed model can be used as a tool to optimize the design of piezoelectric scavengers concerning power and energy density as well as the frequency response. According to results of the simulations the fabricated piezoelectric devices are expected to generate an electrical power in the range of 1-100 µW.

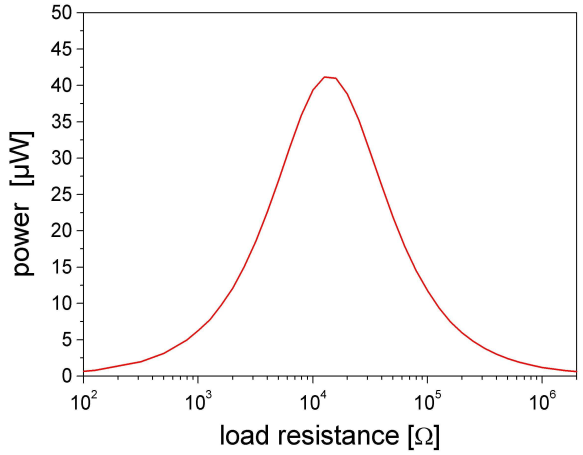

Figure 5.a: Typical characteristics of the output power as a function of the electrical load resistance for a single piezoelectric having a mass of 5x5 mm².

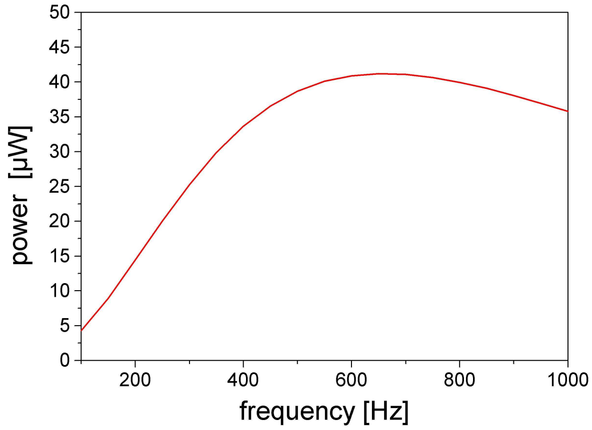

Figure 5.b: Typical characteristics of the output power as a function of the excitation frequency for a single piezoelectric device with a resonance frequency of about 600 Hz..

5 CONCLUSION

A robust MEMS concept for the fabrication and packaging of piezoelectric scavengers was presented. In this process different devices varying in geometric dimensions, resonance frequency and electric connection. are processed on one wafer. The fabrication of the devices is currently ongoing.

Furthermore, a finite element model for this type of piezoelectric generator was developed. According to these simulations the output power is predicted to be in the range of 1 - 100 µW.

ACKNOWLEDGEMENTS

The authors would like to thank the IWT, the Institute for the Promotion of Innovation by Science and Technology in Flanders, Belgium, for sponsoring this research as a part of project SBO 030288 “PowerMEMS”.

6. REFERENCES

[1] M. Strasser, R Aigner, M Franosch, and G Wachutka, 'Miniaturized thermoelectric generators based on poly-si and poly-sige surface micromachining', Journal of Sensors and Actuators, A: Physical, A98-A98:535-542, 2002.

[2] P. Miao, A.S. Holmes, E.M. Yeatman, T.C. Green, and P.D. Mitcheson, 'Micro-machined variable capacitors for power generation', Electrostatics '03, Edinborough, UK, 23-27 March, 2003.

[3] P. Glynne-Jones, M. J. Tudor, S. P. Beeby, and N. M. White, 'An electromagnetic, vibration-powered generator for intelligent sensor systems', Journal of Sensors and Actuators A: Physical, Vol. 110, pp. 344-349, 2004.

[4] N. S. Shenck and J. A. Paradiso, 'Energy scavenging with shoe-mounted piezoelectrics', IEEE Micro, Vol. 21, pp. 30-42, 2001.

[5] M. Umeda, K. Nakamura, and S. Ueha, 'Energy storage characteristics of a piezo-generator using impact induced vibration', Japanese Journal of Applied Physics, Part 1, Vol. 36(5), pp. 3146-3151, 1997.

[6] V. Leonov, P. Fiorini, S. Sedky, T. Torfs and C. van Hoof, 'Thermoelectric MENS generator as a power supply for a body area network', Transducers'05, Proc. of the 13th Intern. conf. on Solid-State Sensors, Actuators and Microsystems, Seoul. Korea, June 5-9, 2005, pp. 291- 294.

[7] T. Sterken, P. Fiorini, K. Baert, R. Puers, G. Borghs, 'An electret-based electrostatic micro-generator', Proc. of Transducers'03, pp. 1291-1294, 2003.

[8] J. Baborowski, 'Microfabrication of piezoelectric MEMS', Journal of Electroceramics, Vol. 12, pp. 33-51, 2004.

[9] N. Ledermann, P. Muralt et al., '{1 0 0}-Textured, piezoelectric Pb(Zr*x*, Ti1−*x*)O3 thin films for MEMS: 'integration, deposition and properties', Journal of Sensors and Actuators A, Vol. 105, pp. 162-170, 2003.

[10] C.G. Xu, T.S. Fiez, 'Nonlinear finite element analysis of a thin piezoelectric laminate for micro power generation', Journal of Microelectromechanical systems, Vol. 12, No. 5, pp. 649-655, 2003.

[11] H.A. Sodano G. Park et al., 'Model of a piezoelectric power harvesting beam', Proc. of IMECE'03, 2003 ASME International Mechanical Engineering Congress, Washington D.C., November 15-21, 2003, pp. 1-10.

[12] M. S.Weinberg, 'Working equations for piezoelectric actuators and sensors', J. Microelectromech. Syst., Vol. 8, pp. 529-533, 1999.